

Y_2O_3 对粒状贝氏体堆焊金属相变和力学性能的影响

邢晓磊¹, 周野飞^{1,2}, 张鹏³, 王吉波¹, 杨育林², 杨庆祥¹

(1. 燕山大学 亚稳材料制备技术国家重点实验室, 河北 秦皇岛 066004;

2. 燕山大学 机械工程学院, 河北 秦皇岛 066004; 3. 神华集团, 河北 秦皇岛 066001)

摘要: 目的 研究稀土氧化物 Y_2O_3 对粒状贝氏体堆焊金属相转变以及力学性能的影响。方法 采用金相显微镜和场发射扫描电镜对堆焊金属的微观组织进行观察, 采用金相显微镜观察并统计出奥氏体晶粒度, 采用 XRD 对堆焊金属表面物相进行测定, 采用显微硬度计和电子万能试验机测量不同 Y_2O_3 质量分数堆焊金属的硬度和拉伸性能, 采用透射电子显微镜对堆焊金属微观结构进行表征。结果 Y_2O_3 能够有效细化堆焊金属的初生奥氏体晶粒, 尺寸由 $51.2\ \mu\text{m}$ 减小到 $40.1\ \mu\text{m}$, 大块先共析铁素体尺寸明显减小, 组织分布均匀, 且 M/A 岛弥散分布。堆焊金属中残余奥氏体相数量随着 Y_2O_3 质量分数的增加而逐渐降低, 马氏体相体积分数增加。 Y_2O_3 的加入明显提升堆焊金属的力学性能, 显微硬度由 (272 ± 13) HV 提升至 (312 ± 8) HV; 抗拉强度由 (764 ± 10) MPa 提升至 (885 ± 12) MPa, 且延伸率增加了 4%。结论 Y_2O_3 的加入能够细化堆焊金属的初生奥氏体晶粒, 促进形成均匀细化的粒状贝氏体组织, M/A 岛的数量逐渐增加, 且 M/A 岛中马氏体相数量增加, 粒状贝氏体堆焊金属的力学性能显著提高。

关键词: 粒状贝氏体; Y_2O_3 ; 初生奥氏体; M/A 岛; 显微硬度; 抗拉强度

中图分类号: TG455 文献标识码: A 文章编号: 1001-3660(2016)04-0017-08

DOI: 10.16490/j.cnki.issn.1001-3660.2016.04.004

Effects of Y_2O_3 on Microstructure and Mechanical Property of Granular Bainite Hardfacing Alloys

XING Xiao-lei¹, ZHOU Ye-fei^{1,2}, ZHANG Peng³, WANG Ji-bo¹, YANG Yu-lin², YANG Qing-xiang¹

(1. State Key Laboratory of Metastable Materials Science & Technology, Yanshan University, Qinhuangdao 066004, China;

2. College of Mechanical Engineering, Yanshan University, Qinhuangdao 066004, China;

3. Shenhua Trading Group Limited, Qinhuangdao 066001, China)

ABSTRACT: **Objective** To investigate the effects of Y_2O_3 additive on the microstructure and mechanical property of granular bainite hardfacing alloy. **Methods** The microstructures of the hardfacing alloy with different Y_2O_3 additives were observed using optical microscopy (OM), scanning electron microscopy (SEM) and transmission electron microscopy (TEM). The phase structures

收稿日期: 2015-11-20; 修订日期: 2016-02-27

Received: 2015-11-20; Revised: 2016-02-27

基金项目: 国家自然科学基金(51271163, 51471148)

Fund: Supported by the National Natural Science Foundation of China (51271163 and 51471148)

作者简介: 邢晓磊(1989—), 男, 博士研究生, 主要研究方向为表面工程。

Biography: XING Xiao-lei (1989—), Male, Ph. D. candidate, Research focus: surface engineering.

通讯作者: 杨庆祥(1962—), 男, 博士, 教授, 主要研究方向为堆焊与表面再制造等。

Corresponding author: YANG Qing-xiang (1962—), Male, Doctor, Professor, Research focus: hardfacing and surface remanufacturing engineering.

of the hardfacing alloys were determined using X-ray diffraction. The hardness, tensile property and abrasive resistance of the hardfacing alloys with different Y_2O_3 additions were determined. **Results** The results showed that the primary austenite in the hardfacing alloy could be refined by Y_2O_3 additive. The grain size of primary austenite decreased from $51.2\ \mu m$ to $40.1\ \mu m$ with the increase of Y_2O_3 addition. Meanwhile, the size of proeutectoid ferrite (PF) decreased significantly and the fraction of the bainite increased, so the M/A island could be distributed uniformly. The XRD analysis showed that the fraction of martensite increased while that of retained austenite decreased with the increase of Y_2O_3 addition. TEM results showed that large number of dislocation martensite was transformed in M/A. The Y_2O_3 additive could improve the hardness, strength and plasticity of the hardfacing alloys. With the increase of Y_2O_3 addition, the hardness increased from $(272\pm13)HV$ to $(312\pm8)HV$, the tensile strength increased from $(764\pm10)MPa$ to $(885\pm12)MPa$ and the elongation increased by 4%. **Conclusion** The grain size of primary austenite decreased with the increase of Y_2O_3 addition. Meanwhile, the PF was refined significantly and M/A islands distributed uniformly. The fraction of martensite increased and the RA decreased with the increase of Y_2O_3 addition. The mechanical property of the hardfacing alloy with Y_2O_3 additive was improved.

KEY WORDS: granular bainite; Y_2O_3 ; austenite; M/A island; Micro-hardness; tensile strength

粒状贝氏体钢以其优异的综合力学性能,广泛应用于制造机械零部件、能源运输用管线和桥梁等^[1-7]。粒状贝氏体由贝氏体铁素体基体和弥散分布的M/A岛(由马氏体与残余奥氏体构成)所组成,其中M/A岛是强化相,可以有效提高钢的强度和韧性^[8-9]。

堆焊技术是表面再制造工程领域中关键技术之一^[10-18]。采用堆焊技术可以修复或再制造报废的齿轮、模具、轧辊等工业零部件^[19-23]。传统的堆焊材料,其堆焊金属主要为马氏体和残余奥氏体组织。Yang等^[23]采用埋弧药芯焊丝制备马氏体堆焊金属对连铸辊进行修复,利用弥散分布的碳化物对堆焊金属进行强化。马氏体和残余奥氏体组织都是亚稳态组织,堆焊后需要采用复杂的热处理工艺,才能保证堆焊金属具有稳定的组织和良好的力学性能^[20],不仅提升了堆焊金属制备的成本,也限制了堆焊再制造的应用。Das Bakshi S等^[24]对马氏体、贝氏体和珠光体三种组织的抵抗磨损性能进行了研究,发现由于马氏体脆性较高,磨损过程中表面层随着磨损的进行会出现大量的剥落,虽然贝氏体和珠光体组织硬度低于马氏体组织,但在磨损过程中,会在其表面形成变形层,有效地提高其耐磨性,减小磨损量。然而,珠光体组织的强度、硬度均相对较低,表面层抵抗变形能力较差。因此,通过抑制珠光体(铁素体)、马氏体转变,获得贝氏体基耐磨金属,在表面再制造中引起了人们的重视^[25-27]。

传统贝氏体钢的制备方法是通过中温等温热处理来获得。但是,堆焊过程是一个空冷过程(连续冷却过程),实现焊后长时间等温转变较困难。所以,如何通过优化合金元素控制堆焊金属的连续冷却曲线

(CCT),以获得粒状贝氏体,受到学者们的广泛关注^[28-30]。Chen等和Guo等^[1,28]通过加入合金元素Mo和Zr,获得了粒状贝氏体,并通过固溶强化作用强化了粒状贝氏体。Qiao等^[8]控制M/A岛数量和形貌尺寸,得到了强韧性良好的力学性能。Wang和Yang等^[29-30]认为增加过冷奥氏体稳定性是提高粒状贝氏体性能较为有效的途径。Chen等^[31]制备了含合金元素V粒状贝氏体组织的堆焊金属,用于再制造钢轨。

目前,稀土元素La、Ce在钢铁材料中的研究已经引起了人们的重视^[32-38]。Warren等^[1]认为 La_2O_3 能够有效改变夹杂物形状,起到变质夹杂的作用。稀土氧化物具有净化钢液的作用,可以与氧、硫结合形成氧硫化物^[35-38,40-41],降低钢中氧硫含量,提高堆焊金属的韧塑性。Wang等^[42]在药芯焊丝中添加了 La_2O_3 ,制备了含粒状贝氏体组织的堆焊金属,发现 La_2O_3 可以提高粒状贝氏体组织的堆焊金属综合力学性能。

近年来,重稀土元素Y由于具有更活泼的化学性质而得到人们的关注^[43-44]。Iulian等^[34]研究了将 Y_2O_3 加入到Stellite 21合金中,发现 Y_2O_3 的加入推动应力诱发相变,提高了Stellite 21合金的耐磨性。Riffard等^[45]采用离子注入的方式将Y注入到304不锈钢表面,发现Y能显著提高304不锈钢在等温氧化实验中的抗氧化性能。目前,还未见稀土元素Y在粒状贝氏体堆焊金属组织中应用的报道。

本文拟自行设计、制备粒状贝氏体堆焊药芯焊丝,在药芯中加入 Y_2O_3 ,研究 Y_2O_3 质量分数对粒状贝氏体堆焊金属焊后冷却过程中相转变规律和力学性能的影响,为稀土元素Y在堆焊金属中的广泛应用提供理论依据。

1 试验

1.1 堆焊金属制备

堆焊母材选用 ASTM 1045 钢。自行制备四组堆焊药芯焊丝,分别在母材上进行堆焊。为了研究 Y_2O_3 对粒状贝氏体堆焊金属的影响,在四组焊丝的药芯中加入质量分数分别为 0%、0.99%、1.96% 和 3.85% 的 Y_2O_3 。

1.2 性能测试及组织观察

堆焊金属成分测定采用 Advant/p-381X 射线荧光光谱仪与 CS-8800 型红外碳硫分析仪,其化学成分(以质量分数计)为: C 0.21% ~ 0.22%, Ni 2.6% ~ 2.65%, Mo 1.25% ~ 1.3%, Mn 0.63% ~ 0.65%, Si 0.83% ~ 0.88%, Al 0.25% ~ 0.26%, Y_2O_3 0%、0.99%、1.96%、3.85%, Fe 余量。

采用 Axiovert 200 MAT 型金相显微镜和日立 S4800-II 场发射扫描电镜对堆焊金属组织形貌进行观察,采用 4% (体积分数) 的 HNO_3 乙醇溶液对试样进行腐蚀,过饱和苦味酸腐蚀堆焊金属原奥氏体晶界,并采用 Image-Pro Plus 软件对奥氏体晶粒度进行统计。采用 D/max-2500/PCX 射线衍射仪对堆焊试

样进行物相分析,X 射线测量范围为 $40^\circ \sim 120^\circ$,测量速度为 $4 (^\circ)/min$ 。采用 FM-ARS 9000 型显微硬度计对试样进行显微硬度测量,测量载荷为 9.8 N。沿直线选取间距为 200 μm 的 10 个点,对各点的硬度进行测量,并求出平均值。采用 INSPEKT TABLE100 型电子万能试验机对堆焊金属的力学性能进行测量。

2 结果及分析

2.1 显微组织

2.1.1 金相组织

图 1 为不同 Y_2O_3 质量分数的堆焊金属在经过相同冷却条件(焊后空冷)下的显微组织。当药芯焊丝中 Y_2O_3 的质量分数为 0% 时,堆焊金属显微组织主要由粒状贝氏体和大块先共析铁素体组成,如图 1a 所示。可以看出,大块先共析铁素体在原奥氏体晶界处析出,且组织非常粗大。随着 Y_2O_3 质量分数的增加,堆焊金属中大块先共析铁素体逐渐消失,堆焊金属组织变得均匀且细小,如图 1b 所示。当 Y_2O_3 的质量分数为 1.99% 时,堆焊金属组织为粒状贝氏体基体上分布着尺寸较为细小的先共析铁素体,如图 1c 所示。堆焊金属组织并没有随 Y_2O_3 质量分数的继续增加而得到进一步细化,如图 1d 所示。

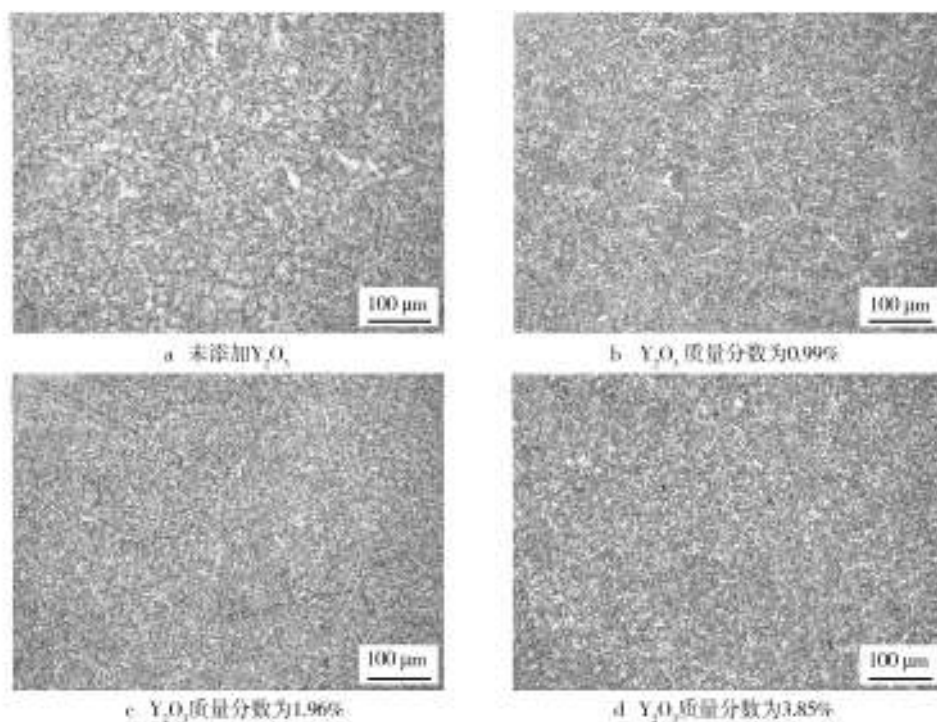


图1 堆焊金属表面显微组织

Fig. 1 Surface microstructures of the hardfacing alloy with different Y_2O_3 additions: a) 0%, b) 0.99%, c) 1.96%, d) 3.85%

2.1.2 XRD

不同 Y_2O_3 质量分数堆焊金属的 XRD 衍射分析结果,如图 2a 所示。可以看出,堆焊金属主要由两相组成,分别为体心立方结构的 α -Fe 相和面心立方结构的 γ -Fe 相。图 2b 为 γ -Fe 衍射峰 γ -111 局部放大,可以看出,随着 Y_2O_3 的加入,残余奥氏体衍射峰强度减弱,说明残余奥氏体相数量减少。图 2c 为 α -Fe 的 α -220 衍射峰放大图,可以看出,随着 Y_2O_3 的加入, α -Fe 的 α -220 衍射峰尖端向小角度方向弯曲。根据布拉格衍射定律,衍射峰向小角度偏移证明该衍射峰所对应相的晶面间距增加。而 α -Fe 的 α -220 衍射峰尖端向小角度偏移,说明体心立方结构有晶面间距不同的两相,证明 M-A 岛中马氏体的相数量随着 Y_2O_3 质量分数的增加而增加。

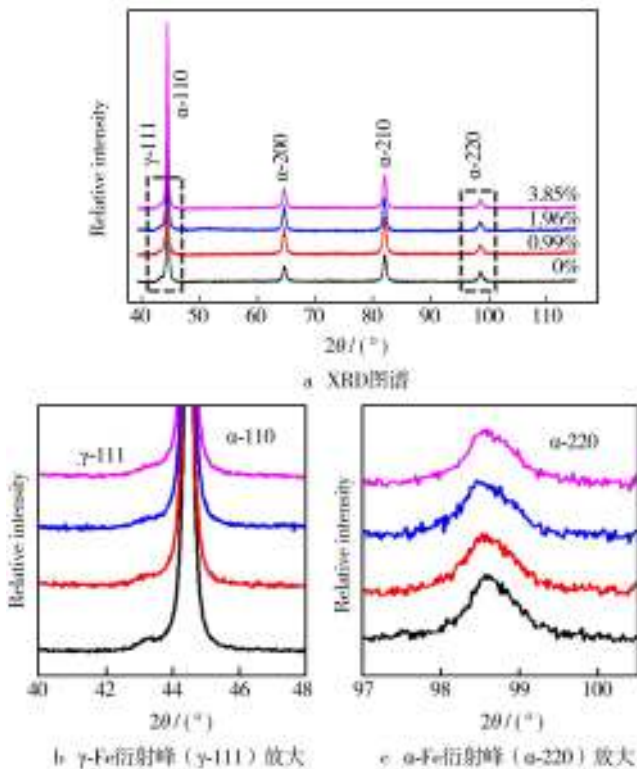


图 2 不同 Y_2O_3 质量分数的堆焊金属 XRD 分析

Fig. 2 XRD patterns of the hardfacing alloys with different Y_2O_3 additions (a) and its amplification of γ -111 diffraction peaks (b) and α -220 diffraction peaks (c)

2.1.3 SEM

图 3 为 Y_2O_3 质量分数为 0% 和 1.96% 时试样的 SEM 形貌。腐蚀效果最明显的是铁素体晶格结构。金相观察到的白色区域为铁素体区,在 SEM 形貌中铁素体为深色区域。大块黑色区域为先共析铁素体,标记为 PF。图 3a 中,在大块 PF 周围分布着贝氏体

(BF)、残余奥氏体(RA)和马氏体-残余奥氏体组成的岛状物(M/A)。加入 Y_2O_3 后,如图 3b 所示,PF 尺寸减小,BF 区域面积和 M/A 岛数量显著增加且分布均匀,显微组织明显细化。

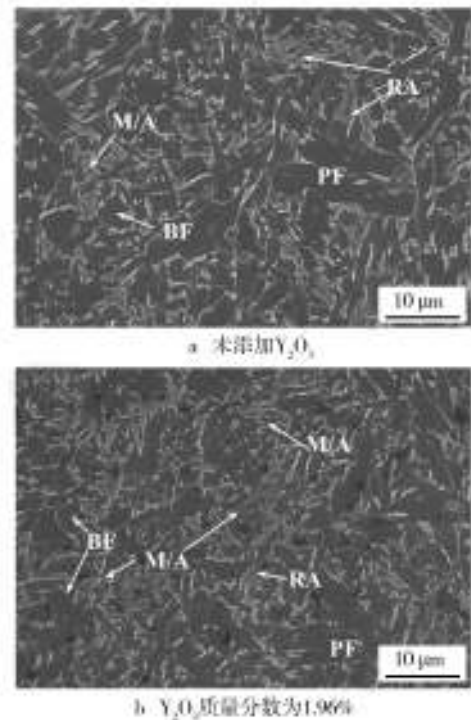


图 3 堆焊金属表面 SEM 形貌

Fig. 3 SEM morphology of the hardfacing metal without (a) and with 1.96wt. % (b) Y_2O_3 additions

2.1.4 奥氏体晶粒度

对原奥氏体的晶粒尺寸进行测量统计,并绘制原奥氏体晶粒尺寸分布图,如图 4 所示。可以看出,当 Y_2O_3 质量分数为 0% 时,堆焊金属的原奥氏体晶粒较粗大,平均尺寸为 $51.2 \mu m$,且晶粒大小不均匀。随着 Y_2O_3 质量分数的增加,堆焊金属的初生奥氏体晶粒尺寸呈现减小的趋势。如图 4c 所示,当 Y_2O_3 质量分数为 1.96% 时,初生奥氏体的晶粒尺寸最小,且初生奥氏体晶粒尺寸分布均匀,平均晶粒尺寸减小到 $40.1 \mu m$ 。继续提高 Y_2O_3 的质量分数,细化效果不再明显。

通过对原奥氏体晶粒尺寸分布的统计发现,随着 Y_2O_3 质量分数的增加,堆焊金属初生奥氏体的晶粒尺寸分布逐渐集中并向小尺寸方向偏移。原奥氏体晶粒变得均匀,尺寸过大或过小的晶粒数量减少。

2.2 力学性能

2.2.1 硬度

图 5 所示为四组堆焊金属表面显微硬度。当

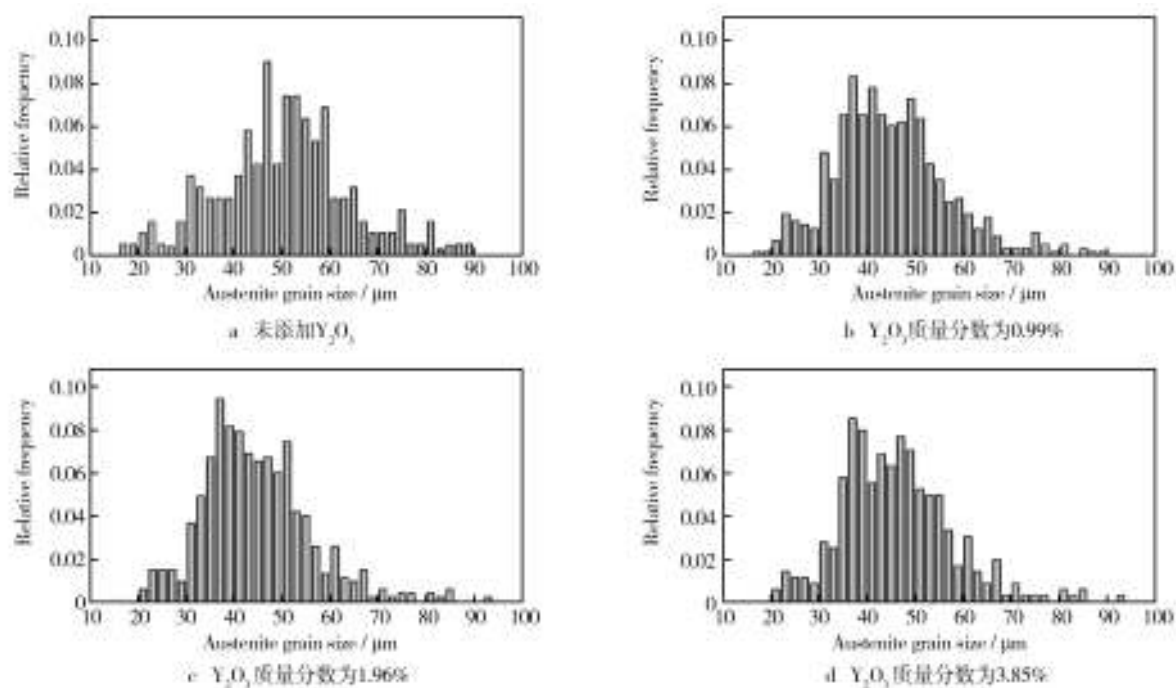


图 4 不同 Y₂O₃ 质量分数堆焊金属原奥氏体晶粒统计

Fig.4 Grain size of austenite in hardfacing metal with different Y₂O₃ additions: a) 0wt. % , b) 0.99wt. % , c) 1.96wt. % , d) 3.85wt. %

Y₂O₃ 质量分数为 0% 时,堆焊金属的显微硬度为(272±13)HV。随着 Y₂O₃ 的加入,堆焊金属显微硬度有了明显的提升,Y₂O₃ 质量分数为 0.99% 时,堆焊金属显微硬度为(295±10)HV。继续提高 Y₂O₃ 的质量分数,堆焊金属显微硬度达到(312±8)HV。Y₂O₃ 的加入明显提高了堆焊金属的硬度,同时堆焊金属表面硬度的均一性也有明显的提升。

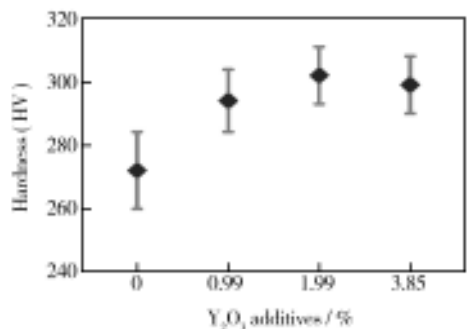


图 5 不同 Y₂O₃ 质量分数的堆焊金属显微硬度

Fig.5 Micro-hardness of the hardfacing alloys with different Y₂O₃ additions

2.2.2 拉伸性能

对 Y₂O₃ 质量分数分别为 0% 和 1.96% 的堆焊金属进行拉伸性能测试。两组堆焊金属拉伸曲线均为连续屈服。当 Y₂O₃ 质量分数为 0% 时,堆焊金属的抗拉强度为 764 MPa,延伸率为 28.5%;当 Y₂O₃ 质量分数为 1.99% 时,堆焊金属的抗拉强度达到 885 MPa,延伸

率提升至 32.5%。可以看出,Y₂O₃ 使得堆焊金属抗拉强度明显提升并且其塑性也有所提升。Y₂O₃ 质量分数分别为 0% 和 1.96% 的堆焊金属拉伸断口表面 SEM 形貌见图 6。对两组试样拉伸断口形貌进行 SEM 观

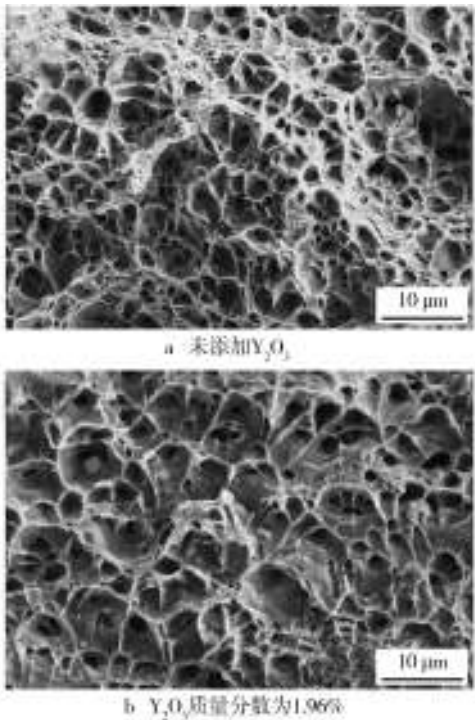


图 6 堆焊金属拉伸断口表面 SEM 形貌

Fig.6 SEM fractographs of the hardfacing alloys: a) 0wt. % , b) 1.96wt. %

察,两组试样断口均由大小不一的韧窝组成,证明两组试样均为典型的韧性断裂。当加入 Y_2O_3 后,堆焊金属断口韧窝深度明显增加,说明其韧性明显提升。

2.3 讨论

堆焊金属在焊后空冷过程中,首先在液相中析出奥氏体,随着温度的下降奥氏体向铁素体转变,过冷奥氏体开始析出先共析铁素体。当堆焊金属温度降至中温区时,部分未转变为先共析铁素体的过冷奥氏体将发生贝氏体转变,形成贝氏体铁素体。固溶在先共析铁素体和贝氏体铁素体中的碳原子,在冷却过程中会向过冷奥氏体中扩散,使得部分区域过冷奥氏体富碳。碳元素的富集能够有效提高过冷奥氏体的稳定性,推迟过冷奥氏体向贝氏体继续转变。当堆焊金属温度降到马氏体转变开始温度(M_s)以下时,部分过冷奥氏体发生马氏体转变。另一部分过冷奥氏体因固溶碳含量过高, M_s 低于室温,这一部分过冷奥氏体最终以残余奥氏体的形式存在。马氏体和残余奥氏体构成了粒状贝氏体中的岛状物(M-A 岛)^[4]。

奥氏体向铁素体转变的过程中经历先共析铁素体形核、铁素体长大两个阶段。先共析铁素体形核: M. Militzer 等^[46]分析了低碳钢中先共析铁素体形成规律,当奥氏体晶粒十分细小或冷却速度较慢的情况下,铁素体只在奥氏体晶粒内部形核,随着晶粒的粗化或冷却速度的增加,奥氏体晶界处会有铁素体晶核形成。Enomoto 和 Aatonson^[47-49]通过研究发现,由于在奥氏体晶粒内部存在较多利于形核的晶体取向,所以铁素体晶核仅在奥氏体晶界个别位置形核。奥氏体晶粒细化会减小晶界处铁素体形核点位置。细化奥氏体能够有效抑制先共析铁素体形核。如图 1 所示,未加入 Y_2O_3 堆焊金属在奥氏体晶界处出现尺寸较大的先共析铁素体。先共析铁素体长大: M. Militzer 等^[46-50]研究发现,先共析铁素体长大开始温度 T_s 与奥氏体晶粒尺寸呈线性关系,随着奥氏体晶粒的细化 T_s 升高,然而 T_s 的提高会显著降低铁素体长大速率,并且合金元素 Mn 的加入会降低碳在奥氏体中的活度,降低相变界面前沿 C 的活度梯度,导致溶质类拖曳效应,碳元素在奥氏体与铁素体晶界前的富集会明显降低铁素体长大速率,扩大奥氏体晶粒度对铁素体长大速率的影响^[46]。M. Militzer 等^[46]通过实验和理论计算证明了先共析铁素体在形成量(50%)相同的条件下,晶粒细化后的奥氏体需要更长的时间完成转变。

先共析铁素体形核数量随着奥氏体晶粒的细化逐渐减少,且晶界处形核点明显减少,而铁素体长大速率随奥氏体晶粒的细化而降低,使得最终形成的铁素体相体积分数有明显的降低,大块先共析铁素体消失。

在未加入 Y_2O_3 的堆焊金属中铁素体相体积分数相对较多,先共析铁素体形成过程中,碳元素不断向未转变的过冷奥氏体中扩散,这就导致堆焊金属在发生贝氏体转变前,过冷奥氏体中固溶的碳含量相对较多,使得在过冷奥氏体向贝氏体铁素体转变过程中相变阻力增加,最终形成贝氏体铁素体的体积分数相对较少,如图 3 所示。碳元素在贝氏体铁素体中固溶量大于先共析铁素体,并且贝氏体铁素体中存在大量的位错,位错能够钉扎碳原子,抑制其进入过冷奥氏体中^[51]。 Y_2O_3 的加入使堆焊金属中贝氏体铁素体相的体积分数增加,导致过冷奥氏体中的碳固溶量降低,当堆焊金属冷却至室温时,部分奥氏体发生马氏体转变,进而增加了 M/A 岛中马氏体相的体积分数。图 7 为 Y_2O_3 质量分数分别为 0% 和 1.99% 的堆焊金属 M/A 岛 TEM,可以清晰地看出 Y_2O_3 加入后,M/A 岛中位错马氏体明显增多,大块残余奥氏体尺寸减小。

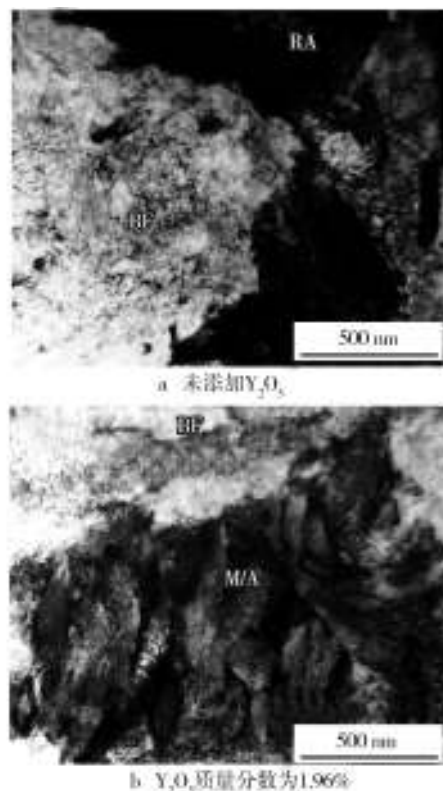


图 7 堆焊金属 TEM 明场像

Fig. 7 TEM morphology of the hardfacing metal without (a) and with 1.96wt. % (b) Y_2O_3 additions

3 结论

本文研究了稀土氧化物 Y_2O_3 对粒状贝氏体堆焊金属相转变以及力学性能的影响。得出以下结论: Y_2O_3 的加入能够细化堆焊金属的初生奥氏体晶粒, 尺寸由 $51.2\ \mu\text{m}$ 减小到 $40.1\ \mu\text{m}$, 并促进形成均匀细化的堆焊金属组织, 大块先共析铁素体消失, M/A 岛弥散分布; 堆焊金属中残余奥氏体相数量随着 Y_2O_3 的加入逐渐降低, 而 M/A 岛的数量逐渐增加, 且 M/A 岛中马氏体相数量增加; Y_2O_3 的加入明显提升了堆焊金属的力学性能, 显微硬度由 $(272 \pm 13)\ \text{HV}$ 提升至 $(312 \pm 8)\ \text{HV}$, 抗拉强度由 $(764 \pm 10)\ \text{MPa}$ 提升至 $(885 \pm 12)\ \text{MPa}$, 延伸率增加了 4%。

参考文献

- [1] CHEN J, TANG S, LIU Z, et al. Influence of Molybdenum Content on Transformation Behavior of High Performance Bridge Steel during Continuous Cooling [J]. *Materials & Design*, 2013, 49: 465—470.
- [2] YAKUBTSOV I A, PORUKS P, BOYD J D. Microstructure and Mechanical Properties of Bainitic Low Carbon High Strength Plate Steels [J]. *Materials Science and Engineering: A*, 2008, 480: 109—116.
- [3] Bhole S D, NEMADE J B, COLLINS L, et al. Effect of Nickel and Molybdenum Additions on Weld Metal Toughness in a Submerged Arc Welded HSLA Line-pipe Steel [J]. *J Mater Process Technol*, 2006, 173: 92—100.
- [4] TSAI Y T, CHANG H T, HUANG B M, et al. Microstructural Characterization of Charpy-impact-tested Nanostructured Bainite [J]. *Materials Characterization*, 2015, 107: 63—72.
- [5] KHODAIE N, IVEY D G, HENEIN H. Extending an Empirical and a Fundamental Bainite Start Model to a Continuously Cooled Microalloyed Steel [J]. *Materials Science and Engineering: A*, 2016, 650: 510—532.
- [6] ZOLOTOREVSKY N Y, PANPURIN S N, ZISMAN A A, et al. Effect of Ausforming and Cooling Condition on the Orientation Relationship in Martensite and Bainite of Low Carbon Steels [J]. *Materials Characterization*, 2015, 107: 278—282.
- [7] LAN L, KONG X, QIU C. Characterization of Coarse Bainite Transformation in Low Carbon Steel during Simulated Welding Thermal Cycles [J]. *Materials Characterization*, 2015, 105: 95—103.
- [8] QIAO Z X, LIU Y C, YU L M, et al. Formation Mechanism of Granular Bainite in a 30CrNi3MoV Steel [J]. *Journal of Alloys and Compounds*, 2009, 475: 560—564.
- [9] WANG S C, HSIEH R I, LIOU H Y. The Effects of Rolling Processes on the Microstructure and Mechanical Properties of Ultralow Carbon Bainitic Steels [J]. *Materials Science and Engineering: A*, 1992, 157: 29—36.
- [10] BUCHELY M F, GUTIERREZ J C, LEÓN L M, et al. The Effect of Microstructure on Abrasive Wear of Hardfacing Alloys [J]. *Wear*, 2005, 259: 52—61.
- [11] CHATTERJEE S, PAL T K. Wear Behaviour of Hardfacing Deposits on Cast Iron [J]. *Wear*, 2003, 255: 417—425.
- [12] KIRCHGABNER M, BADISCH E, FRANEK F. Behaviour of Iron-based Hardfacing Alloys under Abrasion and Impact [J]. *Wear*, 2008, 265: 772—781.
- [13] LIU J, YANG S, XIA W, et al. Microstructure and Wear Resistance Performance of Cu-Ni-Mn Alloy Based Hardfacing Coatings Reinforced by WC Particles [J]. *Journal of Alloys and Compounds*, 2016, 654: 63—70.
- [14] CABROL E, BOHER C, VIDAL V, et al. Plastic Strain of Cobalt-based Hardfacings under Friction Loading [J]. *Wear*, 2015, 330/331: 354—363.
- [15] YANG K, YANG Q, BAO Y. Effect of Carbonitride Precipitates on the Solid/Liquid Erosion Behaviour of Hardfacing Alloy [J]. *Applied Surface Science*, 2013, 284: 540—544.
- [16] CHAKRABORTY G, KUMAR N, DAS C R, et al. Study on Microstructure and Wear Properties of Different Nickel Base Hardfacing Alloys Deposited on Austenitic Stainless Steel [J]. *Surface and Coatings Technology*, 2014, 244: 180—188.
- [17] LAI H H, HSIEH C C, LIN C M, et al. Effect of Oscillating Traverse Welding on Microstructure Evolution and Characteristic of Hypoeutectic Hardfacing Alloy [J]. *Surface and Coatings Technology*, 2014, 239: 233—139.
- [18] HEMMATI I, OCELÍK V, De HOSSON J T M. Dilution Effects in Laser Cladding of Ni-Cr-B-Si-C Hardfacing Alloys [J]. *Materials Letters*, 2012, 84: 69—72.
- [19] LIU C L, LYU Y H, XU B S, et al. Microstructure and Tribological Properties of Layer Deposited by Micro-plasma Arc Welding on Worn Gear [J]. *Surface Engineering*, 2008, 26: 338—341.
- [20] LI D, YANG Y, LIU L, et al. Effects of RE Oxide on the Microstructure of Hardfacing Metal of the Large Gear [J]. *Materials Science and Engineering: A*, 2009, 509: 94—97.
- [21] KASHANI H, AMADEH A, GHASEMI H M. Room and High Temperature Wear Behaviors of Nickel and Cobalt Base Weld Overlay Coatings on Hot Forging Dies [J]. *Wear*, 2007, 262: 800—806.

- [22] VENKATESAN K, SUBRAMANIAN C, SUMMERVILLE E. Three-body Abrasion of Surface Engineered Die Steel at Elevated Temperatures[J]. *Wear*, 1997, 203/204: 129—138.
- [23] YANG K, ZHANG Z X, HU W Q, et al. A New Type of Submerged-arc Flux-cored Wire Used for Hardfacing Continuous Casting Rolls[J]. *J Iron Steel Res Int*, 2011, 18: 74—79.
- [24] DAS BAKSHI S, SHIPWAY P H, BHADOSHIA H K D H. Three-body Abrasive Wear of Fine Pearlite, Nanostructured Bainite and Martensite[J]. *Wear*, 2013, 308: 46—53.
- [25] SAEIDI N, EKRAMI A. Comparison of Mechanical Properties of Martensite/Ferrite and Bainite/Ferrite Dual Phase 4340 Steels[J]. *Materials Science and Engineering: A*, 2009, 523: 125—129.
- [26] BAKHTIARI R, EKRAMI A. The Effect of Bainite Morphology on the Mechanical Properties of a High Bainite Dual Phase (HBDP) Steel[J]. *Materials Science and Engineering: A*, 2009, 525: 159—165.
- [27] Das BAKSHI S, LEIRO A, PRAKASH B, et al. Dry Rolling/Sliding Wear of Nanostructured Bainite[J]. *Wear*, 2014, 316: 70—78.
- [28] GUO J, GUO A, GUO H, et al. Effect of Zirconium Addition on the Austenite Grain Coarsening Behavior and Mechanical Properties of 900 MPa Low Carbon Bainite Steel[J]. *Journal of University of Science and Technology Beijing, Mineral, Metallurgy, Material*, 2008, 15: 688—695.
- [29] WANG J P, YANG Z G, BAI B Z, et al. Grain Refinement and Microstructural Evolution of Grain Boundary Allotriomorphic Ferrite/Granular Bainite Steel after Prior Austenite Deformation[J]. *Materials Science and Engineering: A*, 2004, 369: 112—120.
- [30] YANG H, BHADOSHIA H. Austenite Grain Size and the Martensite-start Temperature[J]. *Scripta Materialia*, 2009, 60: 493—498.
- [31] CHEN J, XING X, WANG Y, et al. Effects of Vanadium Addition on Microstructure and Tribological Performance of Bainite Hardfacing Coatings[J]. *Journal of Materials Engineering and Performance*, 2015, 24: 1157—1164.
- [32] FU H, XIAO Q, KUANG J, et al. Effect of Rare Earth and Titanium Additions on the Microstructures and Properties of Low Carbon Fe-B Cast Steel[J]. *Materials Science and Engineering: A*, 2007, 466: 160—165.
- [33] XUE Y J, JIA X Z, ZHOU Y W, et al. Tribological Performance of Ni-CeO₂ Composite Coatings by Electrodeposition[J]. *Surface and Coatings Technology*, 2006, 200: 5677—5681.
- [34] WANG K L, ZHANG Q B, SUN M L, et al. Microstructural Characteristics of Laser Clad Coatings with Rare Earth Metal Elements[J]. *J Mater Process Technol*, 2003, 139: 448—452.
- [35] WANG L, LIN Q, JI J, et al. New Study Concerning Development of Application of Rare Earth Metals in Steels[J]. *Journal of Alloys and Compounds*, 2006, 408—412: 384—390.
- [36] LI X, ZHOU S, WEI X, et al. Two-wavelength Two-photon Process for Optical Selection of Rare-earth Ions[J]. *Journal of Alloys and Compounds*, 2016, 20: 501—510.
- [37] ZHAO Y, WANG J, ZHOU S, et al. Effects of Rare Earth Addition on Microstructure and Mechanical Properties of a Fe-15Mn-1.5Al-0.6C TWIP Steel[J]. *Materials Science and Engineering: A*, 2014, 608: 106—113.
- [38] CHEN H, LI H Q, SUN Y Z, et al. Microstructure and Properties of Coatings with Rare Earth Formed by DC-plasma Jet Surface Metallurgy[J]. *Surface and Coatings Technology*, 2006, 200: 4741—4746.
- [39] GARRISON W M, MALONEY J L. Lanthanum Additions and the Toughness of Ultra-high Strength Steels and the Determination of Appropriate Lanthanum Additions[J]. *Materials Science and Engineering: A*, 2005, 403: 299—310.
- [40] WANG L M, LIN Q, YUE L J, et al. Study of Application of Rare Earth Elements in Advanced Low Alloy Steels[J]. *Journal of Alloys and Compounds*, 2008, 451: 534—541.
- [41] CAI Y C, LIU R P, WEI Y H, et al. Influence of Y on Microstructures and Mechanical Properties of High Strength Steel Weld Metal[J]. *Materials & Design*, 2014, 62: 83—90.
- [42] WANG Y, CHEN J, YANG J, et al. Effect of La₂O₃ on Granular Bainite Microstructure and Wear Resistance of Hardfacing Layer Metal[J]. *Journal of Rare Earths*, 2014, 32: 83—89.
- [43] ALINGER M J, ODETTE G R, HOELZER D T. On the Role of Alloy Composition and Processing Parameters in Nanocluster Formation and Dispersion Strengthening in Nanostructured Ferritic Alloys[J]. *Acta Materialia*, 2009, 57: 392—406.
- [44] RADU I, LI D Y, LLEWELLYN R. Tribological Behavior of Stellite 21 Modified with Yttrium[J]. *Wear*, 2004, 257: 1154—1166.
- [45] RIFFARD F, BUSCAIL H, CAUDRON E, et al. The Influence of Implanted Yttrium on the Cyclic Oxidation Behaviour of 304 Stainless Steel[J]. *Applied Surface Science*, 2006, 252: 3697—3706.
- [46] MILITZER M, PANDI R, HAWBOLT E B. Ferrite Nucleation and Growth During Continuous Cooling[J]. *Metallurgical and Materials Transactions*, 1996, 27: 1547—1556.

- mary Investigation on Metal Transporting Medium in Vapor Transferring Coating[J]. Surface Technology, 2007, 36(2): 14—15.
- [39] BOROVINSKAYA I, LEVASHOV E A, ROGACHOV A S. Physical-Chemical and Technological Base of Self-propagating High-temperature Synthesis: Course of Lectures [M]. [s. l.]: Moscow Steel and Alloys Institute, 1991.
- [40] KOSTOGOROV P, DOROZHEVETS I N. Transport Reactions in SHS Combustion[J]. International Journal of SHS, 1992, 1: 33—39.
- [41] GKIGOREY Yu M, Merzhanov A G. Combustion Processes in Chemical Technology and Metallurgy [J]. International Journal of SHS, 1992, 1: 600—639.
- [42] 杜心康, 王建江, 尹玉军, 等. 自蔓延高温合成表面涂层技术进展[J]. 材料开发与应用, 2002, 17(2): 34—38.
DU Xin-kang, WANG Jian-jiang, YIN Yu-jun. Development in Surface Coating by Self-propagating High Temperature Synthesis [J]. Development & Application of Materials, 2002, 17(2): 34—38.
- [43] 张卫方, 韩杰才, 陈贵清, 等. 致密 $\text{TiC-Al}_2\text{O}_3\text{-Fe}$ 金属陶瓷的自蔓延高温合成[J]. 复合材料学报, 2000, 17(2): 50—54.
ZHANG Wei-fang, HAN Jie-cai, CHEN Gui-qing, et al. Dense $\text{TiC-Al}_2\text{O}_3\text{-Fe}$ Cermets Fabricated by SHS [J]. Acta Materialia Composita Sinica, 2000, 17(2): 50—54.
- [44] 穆柏春, 刘乘余. 金属表面化学反应陶瓷涂层的研究[J]. 硅酸盐通报, 1997, 16(6): 19—22.
MU Bai-chun, LIU Bing-yu. Research on the Ceramic Coating on Metallic Surface Made by Chemical Reaction Method [J]. Bulletin of The Chinese Ceramic Society, 1997, 16(6): 19—22.
- [45] LICHERI R, ORRU R, CAO G, et al. Self-propagating Combustion Synthesis and Plasma Spraying Deposition of TiC-Fe Powders [J]. Ceramics International, 2003, 29(5): 519—526.
- [46] DALLAIRE S, LEVERT H. Synthesis and Deposition of TiB_2 Containing Materials by Arc Spraying [J]. Surface & Coatings Technology, 1992, 50(3): 241—248.
- [47] VALENTE T, GALLIANO F P. Corrosion Resistance Properties of Reactive Plasma-sprayed Titanium Composite Coatings [J]. Surface & Coatings Technology, 2000, 127(1): 86—92.
- [48] 夏铭, 王泽华, 柏芳, 等. 反应等离子喷涂 TiN 涂层的研究进展[J]. 表面技术, 2015, 44(8): 1—8.
XIA Ming, WANG Ze-hua, BAI Fang, et al. Research Progress of Reactive Plasma Sprayed TiN Coating [J]. Surface Technology, 2015, 44(8): 1—8.
- [49] DONG Yan-chun, YAN Dian-ran, HE Ji-ning, et al. Studies on Composite Coatings Prepared by Plasma Spraying $\text{Fe}_2\text{O}_3\text{-Al}$ Self-reaction Composite Powders [J]. Surface & Coatings Technology, 2004, 179(2): 223—228.
- [50] YAO Yi-hong, WANG Ze-hua, ZHOU Ze-hua, et al. Study on Reactive Atmospheric Plasma-sprayed in situ Titanium Compound Composite Coating [J]. Journal of Thermal Spray Technology, 2013, 22(4): 509—517.
- [51] 刘宏伟, 朱胜, 孙晓峰, 等. 自反应电弧喷涂原位合成 $\text{Ti(C,N)-TiB}_2\text{-Al}_2\text{O}_3$ 复相陶瓷涂层[J]. 中国表面工程, 2013, 26(4): 32—37.
LIU Hong-wei, ZHU Sheng, SUN Xiao-feng, et al. In situ Synthesized $\text{Ti(C,N)-TiB}_2\text{-Al}_2\text{O}_3$ Multi-phased Ceramic Coatings Prepared by Self-reactive Arc Spray Technology [J]. China Surface Engineering, 2013, 26(4): 32—37.
- [52] 王晶, 魏丽凤, 李松湖, 等. AZ31B 镁合金表面自蔓延反应火焰喷涂 Al_2O_3 基陶瓷层的组织结构及性能[J]. 材料保护, 2012, 45(4): 58—59.
WANG Jing, WEI Li-feng, LI Song-hu, et al. Microstructure and Performance of Alumina-matrix Ceramic Coating Prepared on AZ31B Magnesium Alloy by Self Propagating High-temperature Synthesis Reaction Flame Spraying [J]. Materials Protection, 2012, 45(4): 58—62.

(上接第24页)

- [47] ENOMOTO M, AARONSON H I. Nucleation Kinetics of Proeutectoid Ferrite at Austenite Grain Boundaries in Fe-C-X Alloys [J]. Metallurgical Transactions A, 1986, 17: 1385—1397.
- [48] ENOMOTO M, AARONSON H I. On the Critical Nucleus Composition of Ferrite in an Fe-C-Mn Alloy [J]. Metallurgical Transactions A, 1986, 17: 1381—1385.
- [49] ENOMOTO M, LANGE W F, AARONSON H I. The Kinetics of Ferrite Nucleation at Austenite Grain Edges in Fe-C and Fe-C-X Alloys [J]. Metallurgical Transactions A, 1986, 17A: 399—407.
- [50] MILITZER M. Phase Field Modeling of Microstructure Evolution in Steels [J]. Current Opinion in Solid State and Materials Science, 2011, 15: 106—115.
- [51] CABALLERO F, MILLER M, BABU S, et al. Atomic Scale Observations of Bainite Transformation in a High Carbon High Silicon Steel [J]. Acta Materialia, 2007, 55: 381—390.